VER
Vascular & Endovascular Review

# Counteracting Hepatic Fibrosis from CCl4 in Albino Rats Using Epigallocatechin Gallate Extracted from Camellia sinensis

Ali Hadadi1, Sulaiman Alatawi[1], Munirah Almulhim[1], Maryam M. Almousa[1], Adel K. Alkhathami[1], Jawaher Alnahyan[1], Safia I. Aljabr[1], Maryam K. Almuhaysh[1], Abdulaziz Ali Almuarik[1], Abdullah Alanazi[2], Amani M. Marawan*[3], Ahmad M. Moussa[4]

[1]Medical Technologist II, King Abdulaziz Hospital, Al-Ahsa Ministry of National Guard Health Affairs, Saudia Arabia.
[2]Medical Technologist II, Prince Mohammed Bin Abdullaziz Hospital, AL Madinah Ministry of National Guard Health Affairs, Saudia Arabia.
[4]Senior Veterinarian at the General Administration of University Cities, Mansoura University, Egypt, ahmed_moussa@mans.edu.eg

***Contributing Author**
Amani M. Marawan, Fellow of Microbiology, Bacteriology, Immunology and Mycology, Faculty of Veterinary Medicine, Mansoura University, Egypt. Corresponding e-mail: amanielsayed84@mans.edu.eg ; ORCID: https://orcid.org/0000-0001-6343-2669.

## ABSTRACT

The liver plays vital roles in metabolism, excretion, and synthesis necessary for animal health. However, when fibrosis or cirrhosis occurs, these essential physiological functions are compromised. Controlling and halting the progression of liver fibrosis toward cirrhosis is therefore critically important. This study aimed to assess the antifibrotic potential of green tea extract (GTE) against hepatic fibrosis induced by carbon tetrachloride (CCl4) in rats. Sixty male albino rats were divided into four groups: a control group receiving olive oil (1 mL/kg, intraperitoneally) and saline (1 mL/kg/day orally), a CCl4 group receiving 1 mL/kg of CCl4, a group treated with green tea extract (72 mg/kg/day orally), and a group co-treated with both CCl4 and green tea extract. The CCl4 administration resulted in severe hepatotoxicity, evidenced by impaired liver function. Treatment with green tea significantly improved liver function tests and enhanced antioxidant activity. These results indicate that green tea extract, rich in polyphenols, exhibits hepatoprotective and antifibrotic effects in the context of chemically induced liver injury.

**KEYWORDS**: CCL4, Epigallcatechin Gallatin, Hepatic fibrosis, Hepatic stellate cells, Antioxidants..

**How to Cite:** Ali Hadadi1, Sulaiman Alatawi1, Munirah Almulhim1, Maryam M. Almousa1, Adel K. Alkhathami1, Jawaher Alnahyan1, Safia I. Aljabr1, Maryam K. Almuhaysh1, Abdulaziz Ali Almuarik1, Abdullah Alanazi2, Amani M. Marawan*3, Ahmad M. Moussa4, (2025) Counteracting Hepatic Fibrosis from CCl4 in Albino Rats Using Epigallocatechin Gallate Extracted from Camellia sinensis, Vascular and Endovascular Review, Vol.8, No.2s, 32-47.

## INTRODUCTION

Liver diseases represent a major cause of illness and death worldwide in both humans and animals. The development of liver disorders is influenced by a variety of genetic predispositions and environmental factors **(Alaa et al., 2021)**. These diseases are generally classified into hepatocellular, cholestatic, or mixed types. Hepatocellular diseases, which include alcoholic liver disease, non-alcoholic fatty liver disease, viral hepatitis, and toxic hepatitis, predominantly feature liver cell damage, inflammation, and necrosis **(Zhang & Wang, 2020)**. Cholestatic diseases, such as primary biliary cirrhosis, gallstones, and bile duct obstruction, are characterized mainly by impaired bile flow **(Li, J., et al. 2020; Ahmed and Maqbool, 2025)**. Mixed patterns present a combination of hepatocellular and cholestatic injuries, which can be observed in conditions like cholestatic viral hepatitis and drug-induced liver injury **(Shivashankara et al., 2013).**

Green tea, derived from the plant *Camellia sinensis*, is globally consumed and has a long history as a traditional remedy. In recent years, it has gained attention for its potential therapeutic benefits against various human diseases including cardiovascular ailments, diabetes, and cancer **(Kim et al., 2021).** The extract of green tea contains diverse bioactive compounds such as catechins, saponins, and flavonoids. Catechins, in particular, have demonstrated the ability to reduce oxidative stress within cells, lower blood glucose levels, and inhibit cholesterol absorption **(Vinson and Zhang, 2005)**. The hepatoprotective effects of green tea polyphenols are intricately linked to their capacity to decrease lipid peroxidation and oxidative stress **(Lee et al.,2021)**. Furthermore, green tea components mitigate the overproduction of pro-inflammatory cytokines such as interleukins IL-1β and IL-8 **(Kochi et al., 2006)**, along with mediators including Tumor Necrosis Factor-alpha (TNF-α) and Cyclooxygenase-2 (COX-2) **(Tipoe et al., 2010;)**. Additional targets include Platelet-Derived Growth Factor Receptor-beta (PDGF-Rβ), Insulin-like Growth Factor Receptor (IGF-1R) **(Yoichi et al., 2009 and Lee et al., 2021)**, Transforming Growth Factor-beta 1 (TGF-β1), Tissue Inhibitors of Metalloproteinases (TIMP-1 and TIMP-2), and Collagen Type I (Col-I) **(Yan et al., 2013 and Gonzalez et al., 2023)**. Moreover, green tea enhances production of the anti-inflammatory cytokine IL-10 **(Sutherland et al., 2006; Singh et al., 2024)** and attenuates the elevation of specific acute-phase proteins including transferrin, α-1 acid glycoprotein precursor, kallikrein-binding protein, and haptoglobin

**(Guo-Dung et al., 2012 and Chen et al., 2021)**. A recent study revealed that treatment with epigallocatechin-3-gallate (EGCG), the principal catechin in green tea, downregulated several fibrosis-associated signaling pathways in the livers of obese rats, notably the TGF/SMAD **(Cheng et al., 2018)** and PI3K/Akt/FoxO1 pathways **(Singh et al., 2022)**, which are closely implicated in hepatic fibrosis progression**.**

Antioxidant therapy has emerged as a promising approach to prevent and mitigate liver injury and fibrosis. Prior investigations have shown that antioxidants like N-acetylcysteine, vitamin E, silymarin, and quercetin help reduce lipid peroxidation and partially improve liver injury after bile duct ligation (BDL), though their overall effects on fibrosis progression remain debated **(Mona et al., 2012; Patel & Joshi, 2022 and Wang, Z., et al.,2022)**.

In light of conflicting evidence on the hepatic effects of green tea extracts, the current study aims to assess the hepatoprotective properties of green tea extract against carbon tetrachloride ($CCl_4$)-induced liver fibrosis and to explore the underlying protective mechanisms involved.

## MATERIALS AND METHODS

The study utilized sixty male Sprague-Dawley rats, each weighing between 200 and 250 grams. These animals were procured from the Animal Research House affiliated with the Faculty of Veterinary Medicine at Zagazig University. They were housed in transparent plastic cages under controlled environmental conditions, including a temperature maintained around 30°C and a humidity level of 60 ± 10%. The light/dark cycle was set at 12 hours per phase. Rats were provided with standard laboratory feed and unlimited access to fresh water. Before commencing the experiment, the animals were acclimatized for one week. All experimental procedures adhered to ethical guidelines established and approved by the local experimental ethics committee.

## EXPERIMENTAL DESIGN

The rats were randomly allocated into five groups, each comprising 20 animals. Group I served as the control, receiving only 1 mL of 5% carboxymethyl cellulose (CMC) solution orally via gastric gavage for 16 consecutive weeks. Group II was designated as the hepatic fibrosis model, receiving intraperitoneal injections of carbon tetrachloride ($CCl_4$) at 1 mL/kg of a 40% v/v solution in olive oil, administered twice weekly for 16 weeks. In order to simulate clinical conditions more realistically, treatments aimed at fibrosis mitigation were initiated after 8 weeks of $CCl_4$ intoxication and continued concurrently with $CCl_4$ exposure for an additional 8 weeks.

Group III was subjected to $CCl_4$ injections alone for 8 weeks, followed by concurrent administration of $CCl_4$ and green tea extract via oral gavage for another 8 weeks. The green tea extract was administered at a dose of 72 mg/kg/day at a concentration of 7.2% w/v dissolved in saline, with a dosing volume of 1 mL/kg/day. Twenty-four hours following the final $CCl_4$ or treatment dose, blood samples were collected from the medial canthus of the eye for subsequent biochemical and oxidative stress analyses. Liver tissue samples were excised and divided into two portions: one placed in normal saline for preparation of liver homogenates for oxidative stress assays, and the other fixed in 10-15% neutral buffered formalin for histopathological study.

### Sample Preparation

#### Serum Preparation

Collected blood was allowed to clot at room temperature (25°C) for 30 minutes, followed by centrifugation at 2000 g for 10 minutes. The supernatant serum was carefully separated, avoiding disturbance of the buffy coat, and stored in a chilled container until analysis on the same day.

#### Liver Homogenate Preparation

Excised liver specimens were suspended in physiological saline containing heparin (0.16 mg/mL) to prevent coagulation. The tissues were homogenized at 10% w/v concentration in a Tris-HCl buffer (20 mM, pH 7.4) with 1 nM EDTA. The homogenate was centrifuged at 3000 g for 20 minutes at 4°C, and the clear supernatant was collected while avoiding the floating lipid layer. Samples were maintained on ice for immediate biochemical assays.

### Biochemical Assessment

#### Liver Function Tests

Serum alanine aminotransferase (ALT) and aspartate aminotransferase (AST) activities were measured using commercially available kits (Randox, catalog number AL100) following the methods described by Reitman and Frankel (1957). Total bilirubin concentration was determined using the protocol by Pearlman and Lee (1974).

#### Oxidative Stress Markers

Reduced glutathione (GSH) levels were quantified spectrophotometrically in both serum and liver homogenates based on the enzymatic colorimetric method outlined by Beutler et al. (1963). Malondialdehyde (MDA) concentration, indicative of lipid peroxidation, was measured in serum and liver tissue according to the colorimetric assay of Sharma and Wadhawa (1983).

**Histopathological Evaluation of Hepatic Fibrosis**

Periodic core liver biopsies were obtained throughout the experimental timeline, and terminal liver specimens underwent standard histopathological processing. Formalin-fixed tissues were processed using an automated tissue processor (KD-TS6A), involving a two-step fixation-dehydration protocol. Fixation was performed by immersion in 10% neutral buffered formalin for 48 hours, followed by rinsing in distilled water. Dehydration included sequential immersion in graded ethanol concentrations (70%, 90%, and 100%) with exposure times ranging from 90 to 120 minutes per step. After dehydration, tissues were cleared through xylene baths, embedded in paraffin wax, and sectioned at 4–5 µm thickness. Hematoxylin and eosin (H&E) staining was performed according to standard protocols (Suvarna et al., 2013).

**Special Staining**

Masson's trichrome stain was applied on serial sections of the same paraffin blocks to corroborate fibrosis extent and detect minimal fibroproliferative activity potentially undetectable by H&E (Bancroft et al., 1990). This staining also facilitated evaluation of the antifibrotic effects of treatments.

**Immunohistochemical Analysis**

Paraffin sections underwent antigen retrieval via microwaving at 720 W for 25 minutes, followed by overnight incubation at 4°C with primary antibodies targeting transforming growth factor-beta 1 (TGF-β1), alpha-fetoprotein (α-FP), or tumor suppressor protein p53. After PBS washing, sections were incubated with biotinylated secondary antibodies and streptavidin/alkaline phosphatase complexes (Dako Corp.) at 1:200 dilutions. Diaminobenzidine (DAB) was used for chromogenic detection, and counterstaining was performed with hematoxylin. Slides were dehydrated, cleared in xylene, mounted, and examined under high-power light microscopy. Quantification of immunostaining was carried out by measuring the percentage of positively stained areas in seven high-power fields using Image J software (version 1.46a, NIH, USA) (Alaa et al., 2021)

## RESULTS

**Evaluation of Liver Function Tests**

The quantitative analysis of serum alanine aminotransferase (ALT) levels revealed a significant elevation in the group exposed to carbon tetrachloride (CCl4), indicating marked hepatocellular injury compared to the control group. Treatment with epigallocatechin gallate (EGCG) notably reduced ALT levels, showing significant hepatic function improvement relative to the untreated fibrotic group.

Data presented in Table 1 demonstrated that aspartate aminotransferase (AST) levels were markedly increased in the CCl4 group compared to controls and EGCG-treated animals. EGCG administration significantly lowered serum AST, bringing its level close to that seen in controls.

Total bilirubin concentrations were similarly elevated in the CCl4 group versus control. However, no statistically significant differences were observed in bilirubin levels between the EGCG-treated rats and controls (Table 1).

**Antioxidant Activity Improvement by EGCG**

Oxidative stress markers reflected by malondialdehyde (MDA) concentration were significantly raised in the CCl4 group, concomitant with a substantial decrease in the antioxidant glutathione (GSH) in both serum and liver tissues. The group receiving EGCG exhibited a significant reduction in serum and hepatic MDA levels alongside a marked elevation of GSH compared to the CCl4 group (Table 2).

Notably, hepatic GSH content experienced a sharp decline in the CCl4 group but was significantly replenished upon EGCG treatment. Correspondingly, hepatic MDA content showed a significant decrease after EGCG administration, approaching levels observed in the control group.

| Animal Groups | ALT (u/L) | AST (u/L) | Total Bilirubin (mg/dl) |
|---|---|---|---|
| **Control (Group 1)** | $24.25 \pm 4.33^{d}$ | $39.25 \pm 6.14^{d}$ | $0.23 \pm 0.11^{b}$ |
| **Hepatic Fibrosis (Group 2)** | $89.00 \pm 2.65^{a}$ | $100.12 \pm 4.98^{a}$ | $0.61 \pm 0.16^{a}$ |
| **CCl4 + EGCG Treatment (Group 3)** | $31.75 \pm 4.44^{d}$ | $45.00 \pm 3.34^{d}$ | $0.33 \pm 0.86^{b}$ |

*Table 1. Serum liver enzymes and bilirubin levels. Values with different superscript letters are significantly different ($P \leq 0.05$).*

| Animal Groups | GSH (Serum mg/dl) | GSH (Liver mg/g tissue) | MDA (Serum nmol/ml) | MDA (Liver nmol/g tissue) |
|---|---|---|---|---|
| **Control (Group 1)** | $5.28 \pm 0.25^{a}$ | $4.90 \pm 0.33^{a}$ | $3.88 \pm 0.84^{d}$ | $76.72 \pm 2.97^{c}$ |
| **Hepatic Fibrosis (Group 2)** | $0.53 \pm 0.17^{d}$ | $1.05 \pm 0.01^{c}$ | $15.70 \pm 0.38^{a}$ | $100.43 \pm 4.42^{a}$ |
| **CCl4 + EGCG Treatment (Group 3)** | $4.72 \pm 0.18^{a}$ | $4.24 \pm 0.65^{a}$ | $9.25 \pm 0.61^{c}$ | $77.71 \pm 1.66^{c}$ |

***Table 2. Effects of treatments on oxidant and antioxidant markers. Values with different superscript letters differ significantly ($P \leq 0.05$).***

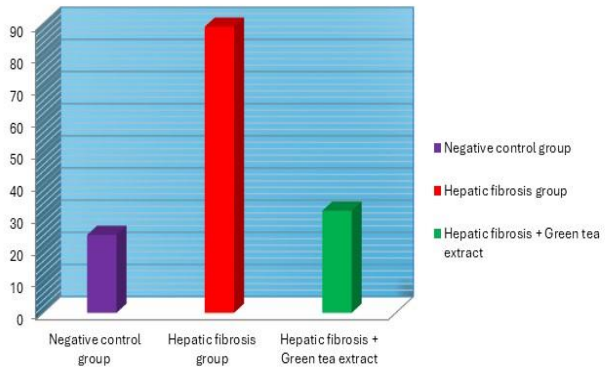


Figure (1): Showing the serum level of ALT in different experimental group

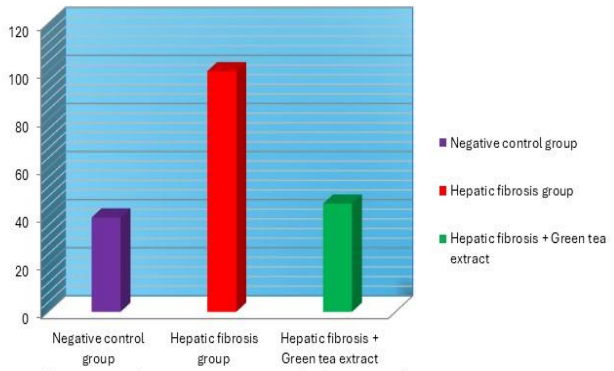


Figure (2): Showing the serum level of AST in different experimental group

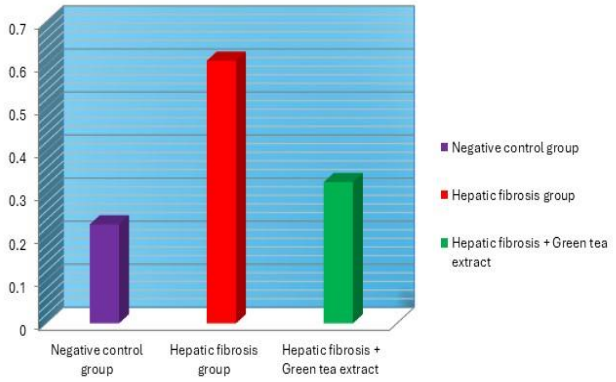


Figure (3): Showing the serum level of total bilirubin in different experimental group.

## Histopathological Findings

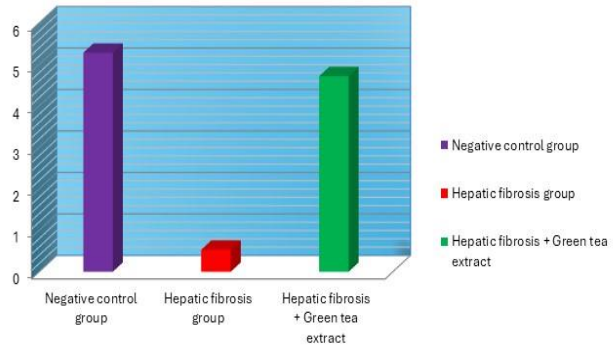


Figure (4): Showing the serum level of reduced glutathione in different experimental group.

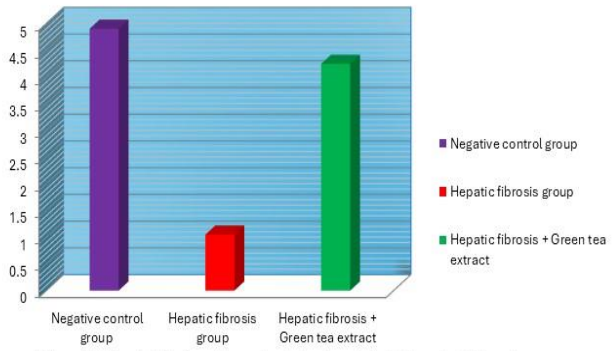


Figure (5): Showing the hepatic content of reduced glutathione in different experimental group.

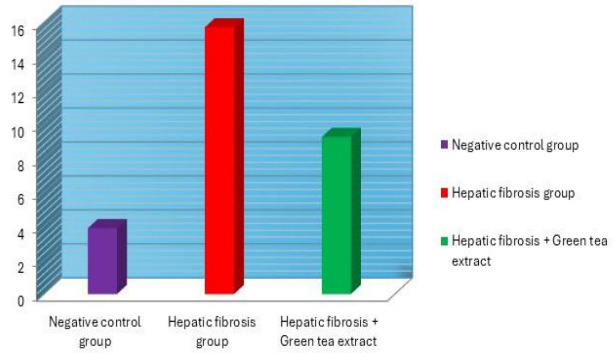


Figure (6): Showing the serum level of malondialdehyde in different experimental group.

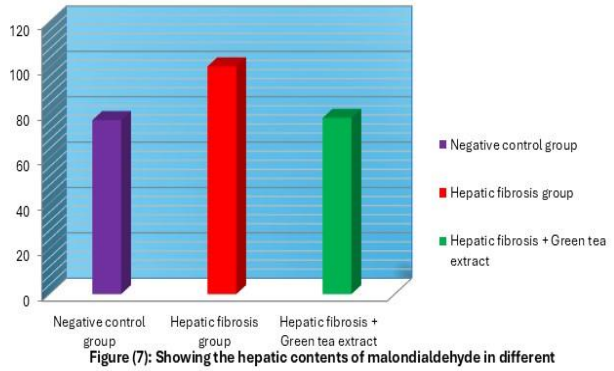


Figure (7): Showing the hepatic contents of malondialdehyde in different experimental group.

Liver sections of hepatic fibrosis group revealed mono-lobular cirrhotic changes represented by fibrous tissue proliferations encircling individual hepatic lobules; most of the hepatic parenchyma was affected with marked portal fibrosis **(figure 9: A, B)**. Each individual lobule showed centrally or eccentrically located central vein and shrinked **(figure, 10)**. Some lobules appeared without central vein. The hepatocytes were large in size with centrally located vesicular nuclei and dense chromatin materials peripherally distributed other hepatocytes were greatly enlarged and the cytoplasm of such cells was

either cloudy, vacuolar, hydropic, fatty or completely disappeared with a few cytoplasmic remnants, in such cases, the nucleus is either pyknotic, necrotic or disappeared **(figure, 11)**. Marked periportal hepatocellular necrosis was evident in some of the examined sections and was represented by empty cytoplasm and centrally or eccentric located nuclei which were mostly pyknotic or karryoretic **(figure, 12)**. Frank coagulative necrosis of hepatocytes was rarely seen and the organization of hepatocytes within the lobules was disrupted (lack of cord organization). The Kupffer cells were mildly or moderately hypertrophied. Some of the hepatic cells were apoptotic **(figure, 13)** and others were regenerated. The portal triads showed mild edema, round cells infiltration (lymphocytes and plasma cells and macrophage) beside biliary and fibroblast proliferations **(figure, 14)**. In some parts of liver, the portal triads showed markedly dilated portal blood vessels and moderate biliary hyperplasia. Portal area also showed dilation of lymphatic vessels. Some of the hepatic lobules suffered peripherolobular macrosteatosis **(figure, 15)** and were extensively surrounded by proliferated fibroblast.

Masson's trichrome stained sections showed marked fibro-cirrhotic changes with their fibrous bands separating the individual hepatic lobules and appeared blue stained. The portal triads showed heavy fibrosis which appeared as a bluish fibrillar martials **(figure, 16: A and B)**. Some fibrous strands were seen extending to the intralobular tissue at a variable distances.

Regarding the treated group with EGCG and $CCl_4$ group, most of the hepatic parenchyma, portal triads and the interlobular septa were apparently normal with minimal remnants of fibrosis around a few hepatic lobules or within the portal triads. The bile ducts were mildly proliferated **(figure, 17)**. A few hepatocytes show mild degenerative changes (cloudy and hydropic degeneration) and/or fatty changes **(figure, 18: A and B)**. The Kupffer cells were hypertrophied and the hepatic sinusoid show variable number of round cells. Characteristic regenerative attempts were seen in a variable number of hepatocytes, such cells appeared large in size with bluish red cytoplasm and enlarged hyper chromatic nuclei and some of these cells were double nucleated **(figure, 19)**. Masson's trichrome stained sections showed a few positively stained fibrous tissue strands around some lobules **(figure, 20)**.

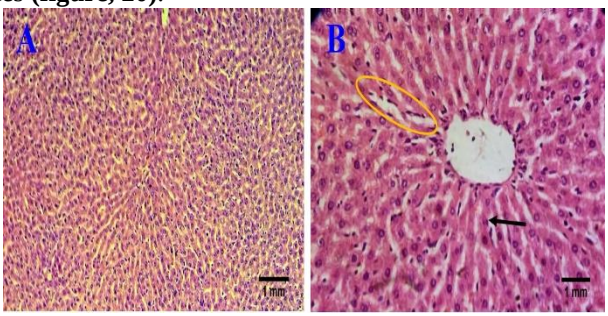


**(Figure, 8) Photomicrograph of rat's liver group (1) showing (A) Normal hepatic architecture (B) High magnification to demonstrate preserved hepatic cords, portal triad's structures, vascular tributaries, biliary system, Von kupffer's cells and supporting stroma. H and E stain, scale bar 1µm.**

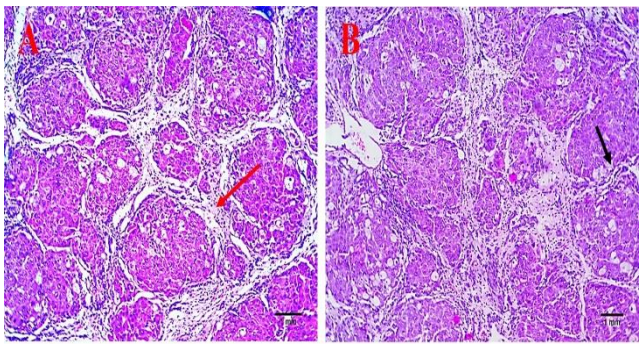


**(Figure, 9) Photomicrograph of rat's liver group (2) showing (A) Monolobular cirrhotic changes with marked portal fibrosis (red arrow) (B) fibrous tissue proliferation encircling the individual hepatic lobule (black arrow). H and E stain, scale bar 1µm.**

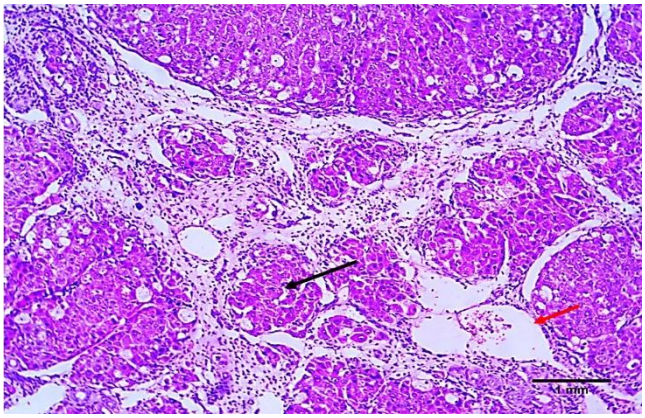

**(Figure, 10) Photomicrograph of rat's liver group (2) showing Hepatic lobule with eccentric central vein (red arrow). Shrinked hepatic lobule without central vein (black arrow). H and E stain, scale bar 1µm.**

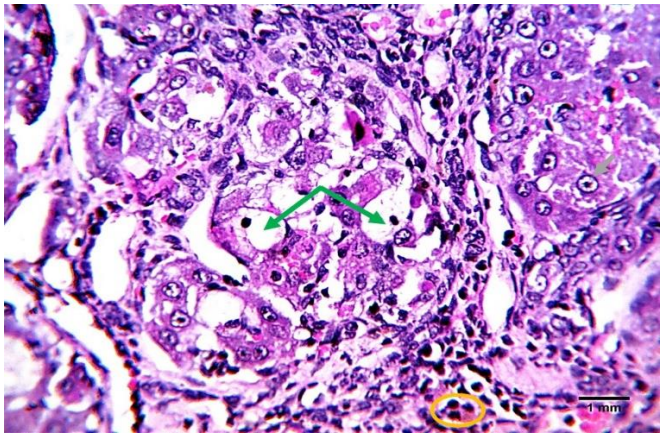

**(Figure, 11) Photomicrograph of rat's liver group (2) showing high magnification to demonstrate hepatocytes with vesicular nuclei and dense chromatin material periphery (gray arrow) or with vacuolar or completely disappeared cytoplasm and pyknotic (green arrows) or necrotic nucleus (yellow circle). H and E stain, scale bar 1µm.**

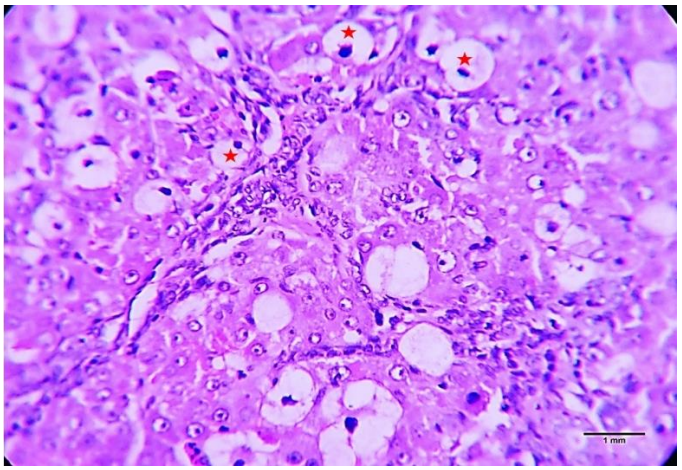

**(Figure, 12) Photomicrograph of rat's liver group (2) showing high magnification to demonstrate periportal hepatocellular necrosis represented by empty cytoplasm and pyknotic or karryoretic nucleus (red stars). H and E stain, scale bar 1µm.**

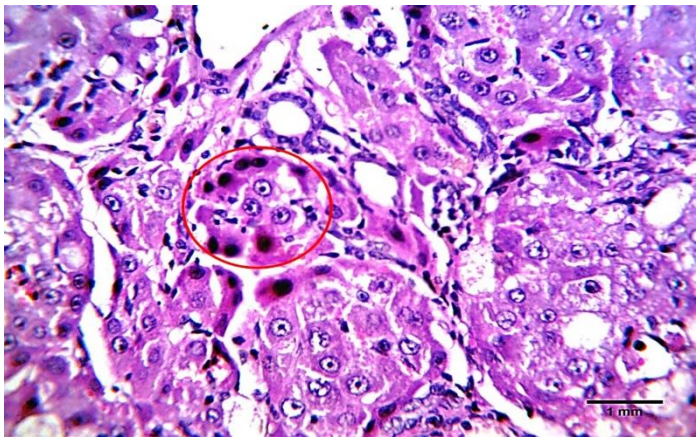

**(Figure, 13) Photomicrograph of rat's liver group (2) showing high magnification to demonstrate some apoptic hepatocytes (red circle). ). H and E stain, scale bar 1µm.**

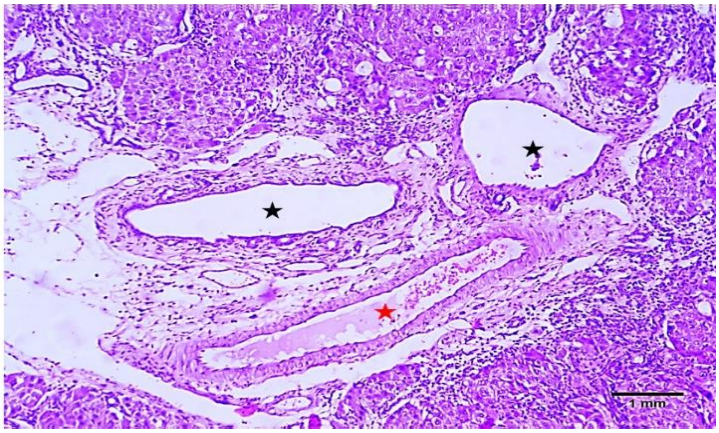

**(Figure, 14) Photomicrograph of rat's liver group (2) showing high magnification to demonstrate marked dilated portal blood vessels (black stars) and moderate biliary hyperplasia (red star). H and E stain, scale bar 1µm.**

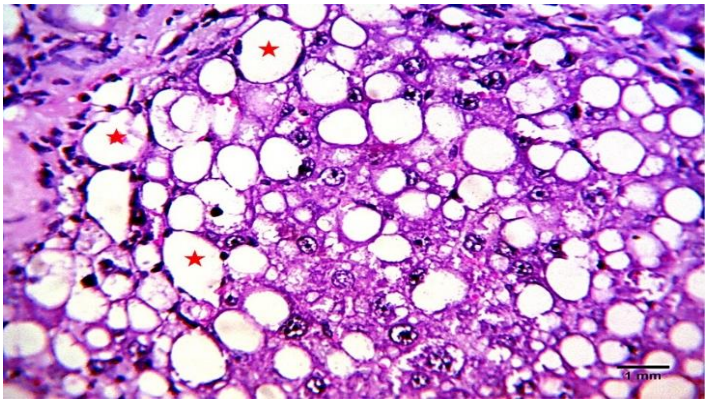

**(Figure, 15) Photomicrograph of rat's liver group (2) showing high magnification to demonstrate the peripherolobular macrosteatosis in some hepatic lobules (red stars). H and E stain, scale bar 1µm.**

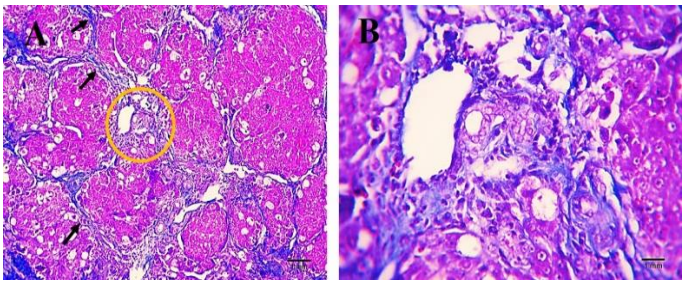


**(Figure, 16) Photomicrograph of rat's liver group (2) showing (A) marked fibro-cirrhotic changes with fibrous strands separating the individual hepatic lobules (black arrows) (B) High magnification to demonstrate heavy fibrosis in portal triads (orange circle in slide A). Masson trichrome stain, scale bar 1µm.**

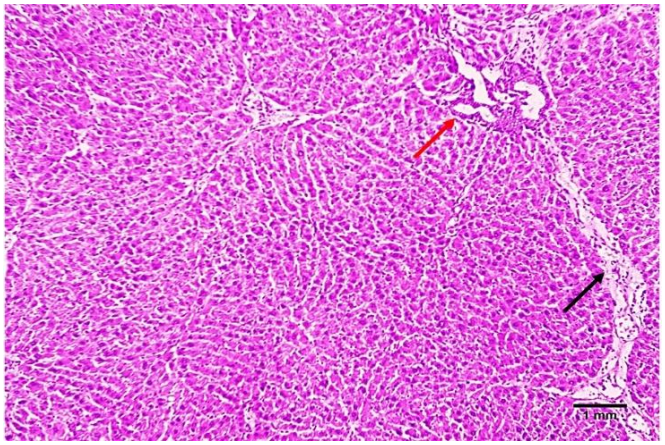

**(Figure, 17) Photomicrograph of rat's liver group (3) showing apparently normal hepatic parenchyma and portal triads with mild proliferated bile duct (red arrow) with minimal remnant of fibrosis around few hepatic lobules (black arrow). H and E stain, scale bar 1µm.**

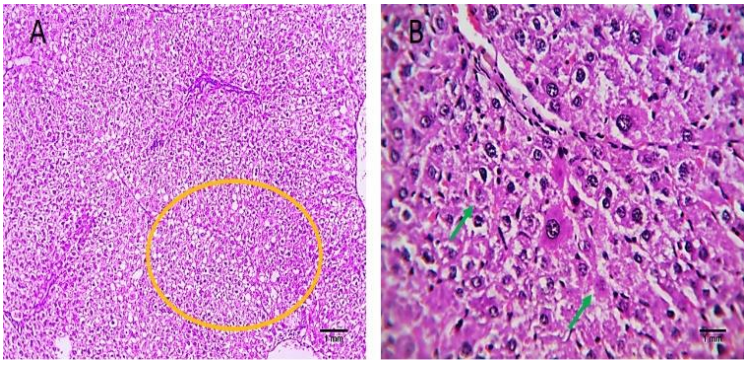


**(Figure, 18) Photomicrograph of rat's liver group (3) showing (A) few hepatocytes showing fatty change (yellow circle) (B) High magnification to demonstrate the mild degenerative changes in hepatocytes (cloudy and hydropic degeneration) (green arrows). H and E stain, scale bar 1µm.**

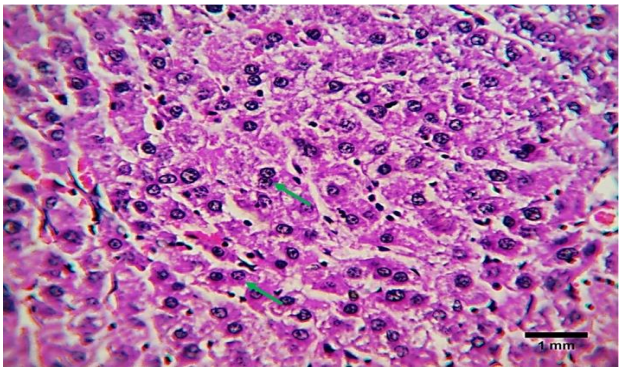

**(Figure, 19) Photomicrograph of rat's liver group (3) showing High magnification to demonstrate some hepatocytes of large size, with bluish red cytoplasm and enlarged hyperchromatic nuclei (green arrows). H and E stain, scale bar 1µm.**

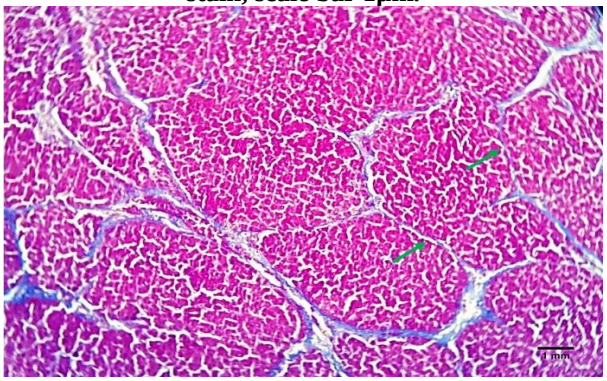

**(Figure, 20) Photomicrograph of rat's liver group (3) showing positively stained fibrous tissue materials around some hepatic lobules (green arrows). Masson's trichrome stain, scale bar 1µm.**

**Hepatic Immunohistochemical staining:**

All of the hepatic cells showed negative stainability for αFP, TGF-$\beta_1$ and P53 in the negative control group **(figure,21: A and B, figure 22 (A& B) and figure 23**) while in hepatic fibrosis group, for αFP about 1-3% of the stromal cells and the regenerated hepatic cells showed positive cytoplasmic brownish stainability, the remaining cells of the liver were negatively stained **(figure, 24 (A & B),)**. Moreover, for TGF-$\beta_1$, nearly 3-5% of the peripherolobular hepatocytes showed positive brownish cytoplasmic stain ability. The positively stained stromal cells were variable and ranged between 15-20% of the proliferating stromal cells while the remaining parenchymal cells were normal and the round cells in addition to the mature fibroblast cells were negatively stained. The proliferating vascular endothelial cells were positively stained for TGF-$\beta_1$ **(figure, 25: A and B)**. Additionally, for P53, roughly 8-10% of the hepatocytes and stromal cells showed small apoptotic cells with deep brownish stained cytoplasm and small condensed nuclei **(figure, 26: A and B)**.

The treatment group with EGCG showed for αFP about 13-15% of the hepatic parenchyma and stromal cells showed positive brownish cytoplasmic stainability for αFP. Most positive cells were located peripherolobular or periportal **(figure, 27: A and B)**. For TGF-$\beta_1$, about 10-12% of the regenerating hepatocytes and 13-15% of the proliferated stromal cells (fibroblast and macrophage) were positively stained. Some of the endothelial cells of the portal blood vessels were also positively stained **(figure, 28: A and B)**. Additionally, from 1-2% of the parenchymal and stromal cells showed positive cytoplasmic stainability for P53 **(figure, 29)**.

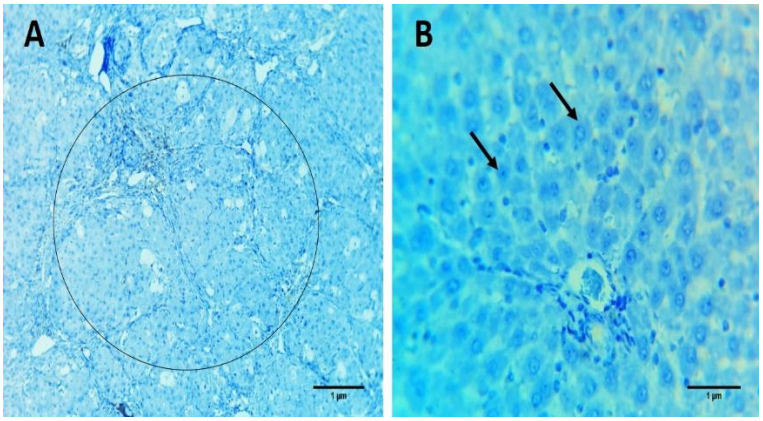


**(Figure, 21): Photomicrograph of rat's liver of group (1) showing (A) All hepatic cells showing negative stainability for αFP. Immunohistochemical stain for αFP, scale bar 1µm (B) High magnification to demonstrate the negative stainability of the hepatocytes. Immunohistochemical stain for αFP, scale bar 1µm.**

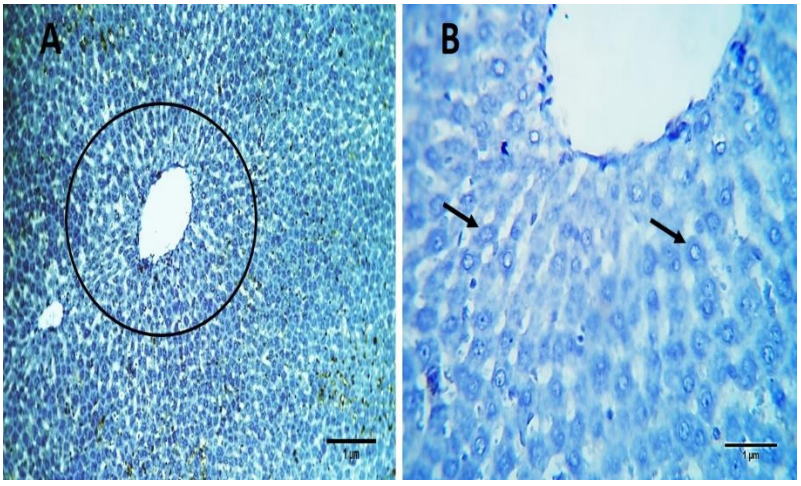


**(Figure, 22): Photomicrograph of rat's liver of group (1) showing (A) the hepatocytes and the vascular structure of portal triads showing negative stainability for TGF-β1. Immunohistochemical stain for TGF-β1, scale bar 1µm. (B) High magnification to demonstrate the negative stainability of the hepatocytes. Immunohistochemical stain for TGF-β1, scale bar 1µm.**

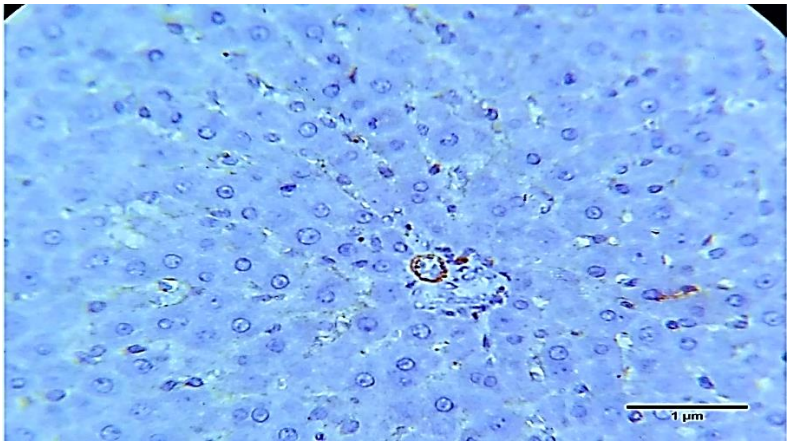


**(Figure, 23): Photomicrograph of rat's liver of group (1) showing Expressions of P53 in 1-2% of the hepatocytes in some hepatic lobules (black circle). Immunohistochemical stain for P53, scale bar 1µm.**

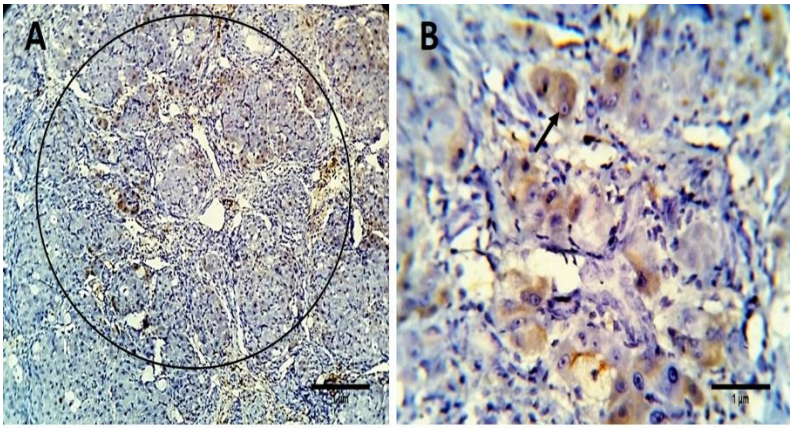


**(Figure, 24): Photomicrograph of rat's liver of group (2) showing (A) Expression of αFP in 1-3% of the stromal cells and regenerated hepatocytes. Immunohistochemical stain for αFP (black circles), scale bar 1µm. (B) High magnification to demonstrate the brownish stainability of the positive cells (black arrows). Immunohistochemical stain for αFP, scale bar 1µm.**

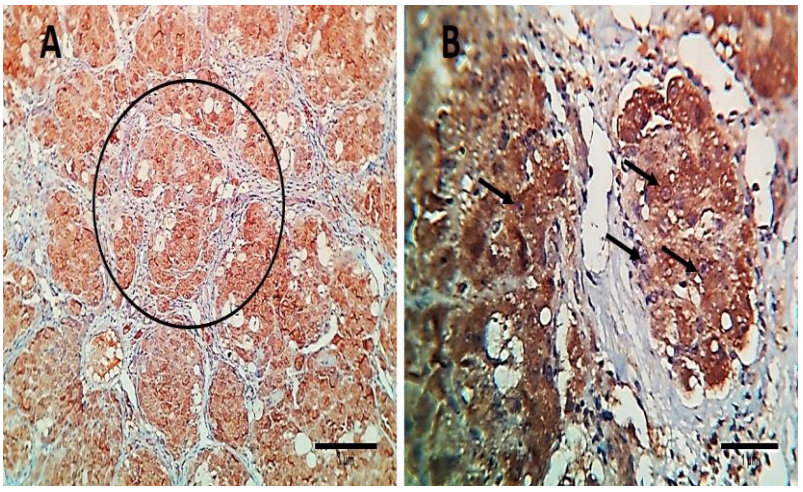


**(Figure, 25): Photomicrograph of rat's liver of group (2) showing (A) Expression of TGF-β1 in 15-20 % of the hepatic parenchyma and stromal cells. Immunohistochemical stain for TGF-β1 (black circles), scale bar 1µm. (B) High magnification to demonstrate the brownish stainability of the positive cells (black arrows). Immunohistochemical stain for TGF-β1, scale bar 1µm.**

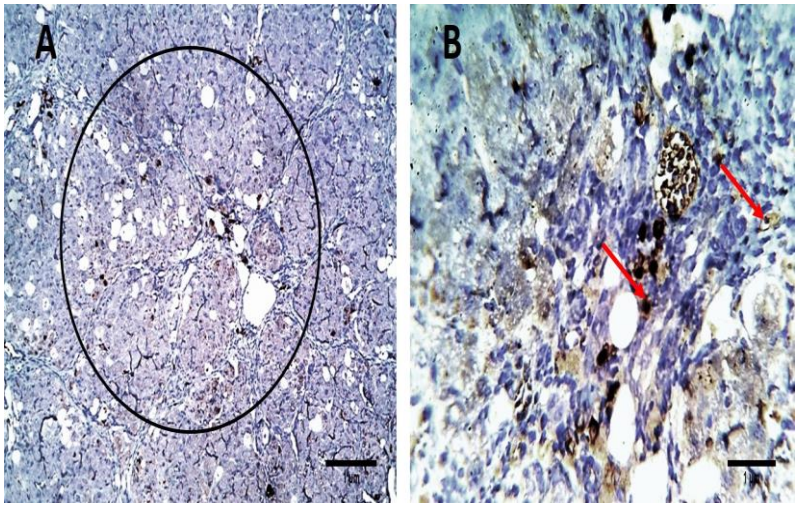


**(Figure, 26): Photomicrograph of rat's liver of group (2) showing (A) Expression of P53in 8-10% of the hepatocytes and stromal cells. Immunohistochemical stain for P53 (black circle), scale bar 1µm. (B) High magnification to demonstrate the brownish stainability of the positive cells (red arrows). Immunohistochemical stain for P53, scale bar 1µm.**

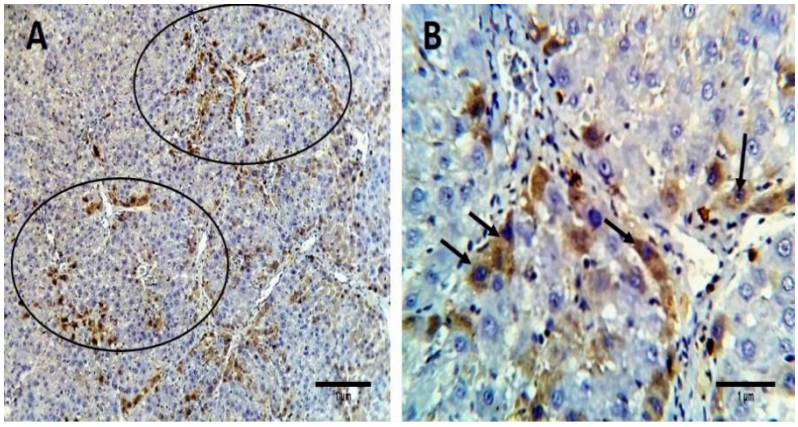


**(Figure, 27): Photomicrograph of rat's liver of group (3) showing (A) Expression of αFP in 13-15% of the hepatic parenchyma and stromal cells. Immunohistochemical stain for αFP (black circles), scale bar 1µm. (B) High magnification to demonstrate the brownish stainability of the positive cells (black arrows). Immunohistochemical stain for αFP, scale bar 1µm.**

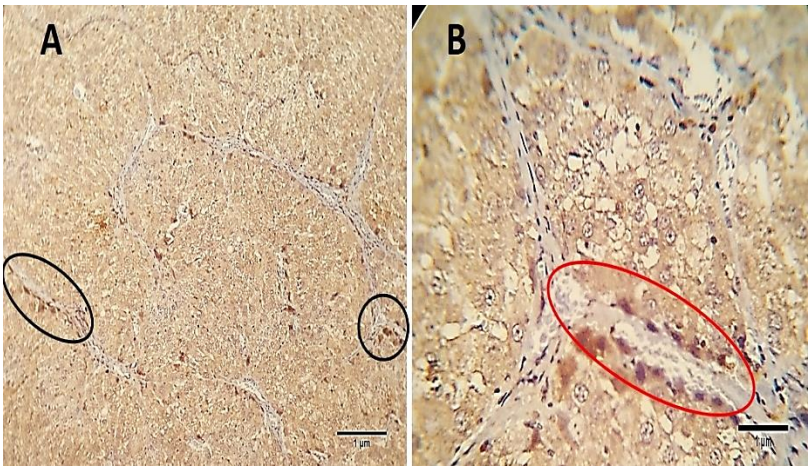


**(Figure, 28): Photomicrograph of rat's liver of group (3) showing (A) Expression of TGF-β1 in 10-12% of the regenerating hepatocytes and 13-15% of the proliferated stromal cells. Immunohistochemical stain for TGF-β1 (black circles), scale bar 1µm. (B) High magnification to demonstrate the brownish stainability of the positive cells (red circle). Immunohistochemical stain for TGF-β1, scale bar 1µm.**

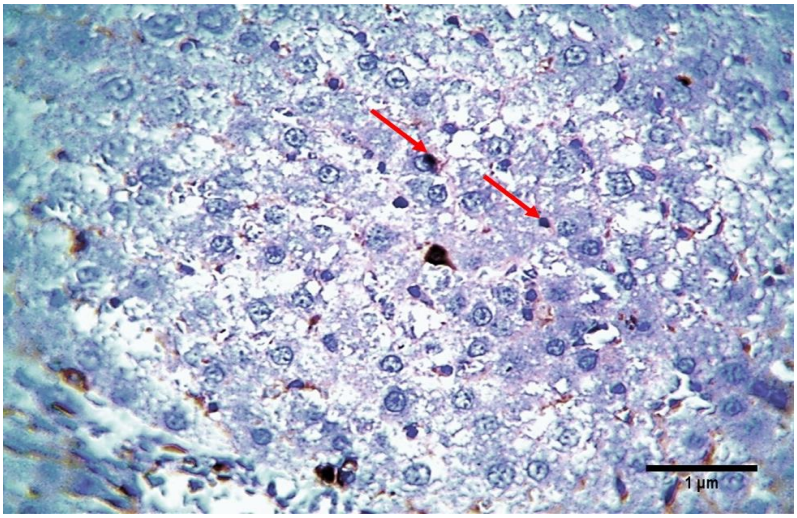


**(Figure, 29): Photomicrograph of rat's liver of group (3) showing Expressions of P53 in 1-2% of the parenchymal and stromal cells (red arrow). Immunohistochemical stain for P53, scale bar 1µm.**

## DISCUSSION

Green tea, derived from *Camellia sinensis* of the *Theaceae* family, is widely acknowledged for its therapeutic potential in mitigating liver fibrosis. The hepatoprotective properties of green tea extract (GTE) have been evidenced against a broad spectrum of toxic insults, including industrial chemicals such as 2-naphthoquinone **(Mahmoud et al., 2012).** The primary bioactive components responsible for these effects are catechins and their derivatives, notably epicatechin (EC), epicatechin gallate (ECG), epigallocatechin (EGC), and most prominently, epigallocatechin-3-gallate (EGCG), which is recognized as the major and most potent antioxidant in green tea **(Wang and Ho, 2009 and Li et al., 2023).**

In this investigation, histopathological analyses unequivocally revealed that GTE administration substantially alleviates liver fibrosis. The observed fibrotic alterations were reduced to minimal residual fibrous tissue localized around a limited number of hepatic lobules or portal triads. Mild biliary epithelial hyperplasia, modest degenerative hepatocellular changes, Kupffer cell hypertrophy, infiltration of mononuclear cells, and evident hepatocyte regeneration characterized the hepatic morphology in treated rats. These findings are attributable to the antioxidant efficacy of green tea catechins, which is mediated primarily through hydroxyl groups on their benzene ring structures; EGCG, in particular, exhibits the strongest free radical scavenging activity **(Wang et al., 2022)**. This potent antioxidative effect is underpinned by the unique molecular architecture of EGCG, containing multiple hydroxyl groups arranged as catechol, gallate, and additional hydroxyl moieties, each conferring hydrogen-donating capacity that effectively neutralizes diverse reactive oxygen species, including the highly reactive hydroxyl radicals initiating lipid peroxidation processes **(Frie and Higdon, 2003; Patel and Joshi, 2022; Rao et al., 2024).**

Recent research elucidates an additional antifibrotic mechanism involving EGCG's modulation of the renin-angiotensin system (RAS) **(Chen and Liu, 2024)**. The RAS, an endocrine regulatory axis, plays a central role in controlling intrahepatic vascular resistance, with angiotensin II (Ang II) serving as its principal effector. Ang II is generated either via endothelial conversion of angiotensin I (produced by hepatocytes from angiotensinogen) or synthesized locally within damaged hepatic tissues **(Munshi et al., 2011; Ahmad et al., 2014).**

***Kochi et al. (2014)*** demonstrated that RAS activation significantly contributes to liver fibrosis progression in obese and hypertensive rat models, wherein EGCG exerts antifibrotic effects by decreasing Ang II concentrations and suppressing hepatic expression of angiotensin-converting enzymes (ACE) and angiotensin II type 1 receptor (AT-1R) mRNA. Ang II directly promotes fibroblast activation by stimulating transforming growth factor-beta 1 (TGF-β1) expression and enhancing collagen synthesis through AT-1R activation **(Manar et al., 2014; Chen and Liu, 2024)**.

Pharmacological blockade of Ang II production or its interaction with AT-1R inhibits hepatic stellate cell (HSC) activation, reduces tumor necrosis factor-alpha (TNF-α) production, diminishes oxidative stress, and thereby attenuates fibrosis development within chronic hepatic injury experimental models **(Hirose et al., 2007)**. Targeted delivery of AT-1R antagonists specifically to activated HSCs is effective in mitigating inflammation and advanced liver fibrosis in rodents **(Moreno et al., 2010)**. Corroborating these findings, the present study proposes that GTE, via its EGCG content, mitigates liver fibrosis by downregulating hepatic inflammation, systemic oxidative stress, and lipid peroxidation associated with RAS activation.

Immunohistochemical analyses focusing on apoptotic markers revealed a significant decrease in the ratio of apoptotic cells to total hepatic cells, marked by lowered p53 expression in EGCG-treated groups compared to the CCl4-intoxicated group.

Though the variance between treatment cohorts was not statistically significant, the data imply an anti-apoptotic role for green tea polyphenols. EGCG's inhibition of hepatocyte apoptosis post-CCl4 exposure is mediated through a p53-dependent mitochondrial pathway, potentially retarding fibrosis progression **(Rania et al., 2015; Zhao et al., 2024)**.

The most notable reduction in fibrosis severity was evident in EGCG-treated animals (group 3), consistent with studies indicating that EGCG suppresses HSC activation, reduces concentrations of fibrogenic mediators, and limits collagen accumulation through its antioxidant properties **(Yasuda et al., 2009; Tipoe et al., 2010; Manar et al., 2014; Chen et al., 2025)**. Previous research supports that decaffeinated GTE administration with $CCl_4$ effectively prevents hepatic fibrosis and collagen deposition **(Hung et al., 2012; Mahmoud et al., 2012; Tsai et al., 2013; Kim et al., 2021)**. Similarly, GTE has been shown to significantly reduce immunoreactive areas of α-smooth muscle actin (α-SMA) and TGF-β1, markers indicative of fibrogenic activity **(Kobayashi et al., 2010; Zhang and Wang, 2020; Lee et al.,2021; Singh et al., 2024)**. Although the precise molecular pathways underlying GTE's therapeutic effects remain to be fully unveiled, it is plausible that its antifibrotic efficacy is derived from combined antioxidant and anti-apoptotic mechanisms, which counteract oxidative stress and apoptosis linked to lipopolysaccharide (LPS)-induced hepatic cell damage **(Ahmed et al., 2017; Lee et al., 2021; Li et al., 2025)**.

Administering GTE at a dose of 72 mg/kg/day concurrently with $CCl_4$ for two months notably suppressed the elevated serum levels of AST and ALT induced by $CCl_4$, restoring enzyme levels toward those observed in untreated controls. This suggests that GTE facilitates stabilization of hepatic cell membranes and promotes structural repair of $CCl_4$-mediated injury **(Karakus et al., 2011; Manar et al., 2014; Li et al., 2020; Chen et al., 2025)**.

Total bilirubin levels decreased significantly following treatment, although intergroup comparisons were not statistically significant. Recovery of hepatic parenchyma and regeneration of hepatocytes generally correspond with normalization of plasma transaminases **(Thabrew et al., 1987; Chen et al., 2021).**

Additionally, GTE administration significantly modulated the extent of oxidative stress induced by $CCl_4$ toxicity. The reduction in serum and hepatic malondialdehyde (MDA) levels signifies inhibition of lipid peroxidation, while increased glutathione (GSH) levels denote enhanced antioxidant defense. These observations align with earlier reports affirming GTE's protective capacity in diminishing oxidative stress markers and elevating GSH content during $CCl_4$-induced hepatic oxidative injury **(Mahmoud et al., 2012; Tsai et al., 2013; Manar et al., 2014; Eman et al., 2012)**. Findings indicate EGCG's active contribution to the hepatoprotective mechanism predominantly through antioxidant action, as reflected in improved serum and hepatic lipid peroxidation parameters **(Omima and Abeer, 2008; Patel and Joshi, 2022; Li et al., 2025)**. The significant enhancement of serum and liver GSH likely results from upregulation of intrinsic hepatic antioxidant activity, mediated by GTE's strong free radical scavenging profile due to its polyphenolic constituents **(Chen et al., 2021; Johnsonet al., 2025).**

Polyphenol profiling by liquid chromatography revealed catechin as the predominant compound within GTE (31.8 mg/g), followed by pyrogallol (21.8 mg/g), naringenin (11.9 mg/g), catechol (10.9 mg/g), and epicatechin (10.5 mg/g), alongside minor quantities of additional phenolics such as vanillic, syringic, salicylic, benzoic, ferulic, coumaric, and cinnamic acids. These results exhibit variability compared to previous studies reporting catechins constitute 30-36% of total GTE dry weight, with EGCG representing up to 63% **(Roomi et al., 2016; Li et al., 2025)**. The protective effects attributed to green tea arise largely from polyphenolics and tannic acid, known for their substantial antioxidant activities against oxidative free radicals **(Tomaszewska et al., 2015; Gramza et al., 2005; Wang et al., 2022).**

Evaluation of GTE's radical scavenging potential using DPPH and β-carotene assays revealed potent free radical neutralization capacity—92.62% DPPH inhibition and β-carotene inhibition of 88.3% and 97.6% at concentrations of 500 and 1000 μg/mL, respectively—indicating effective lipid peroxidation chain-breaking activity. These findings are consistent with prior reports highlighting GTE's capacity to scavenge free radicals **(Panat et al., 2016; Rao et al. 2024)**.

## CONCLUSION

This comprehensive study highlights that treatment and potential reversal of liver fibrosis are achievable objectives with the utilization of GTE. The polyphenolic constituents of GTE, notably EGCG, confer a multifaceted protective role by exerting potent free radical scavenging activity, downregulating inflammatory cytokines and pro-apoptotic mediators, promoting improved hepatic microcirculation, and suppressing extracellular matrix production. The hepatoprotective and antifibrotic mechanisms of GTE involve direct antioxidant effects of absorbed polyphenols, enhancement of endogenous cytoprotective pathways including increased antioxidant mediators (heme oxygenase-1, glutathione), DNA repair activation, anti-apoptotic modulation through p53-related pathways, and inhibition of hepatic stellate cell activation coupled with diminished profibrogenic signaling and collagen matrix deposition.

**Acknowledgments**: We would like to acknowledge the contributions of researchers whose work has been cited in this manuscript.

**Authorship contribution statement**

**Ali Hadadi, Sulaiman Alatawi, Munirah Almulhim, and Maryam M. Almousa**: Visualization, Methodology, Validation, Investigation, and Formal Analysis. **Adel K. Alkhathami, Jawaher Alnahyan, Safia I. Aljabr**: Methodology, Validation, Investigation, **Maryam K. Almuhaysh, Abdullah Alanazi, Abdulaziz Ali Almuarik**: Investigation, Methodology, editing, Resources, Writing. **Amani E. Marawan:** Writing original draft, Analysis, Methodology, Resources, and editing; **Ahmad M. Moussa:** Conceptualization, Analysis, Supervision, Methodology, Resources, Editing, and Writing.

**Data availability**

Data are available from the corresponding author on reasonable request.

**Funding sources:** No funding.

**Declaration of competing interest:** The authors declare that they have no known competing financial interests or personal relationships that could have appeared to influence the work reported in this paper.

**Ethical of approval:** The ethical approval has been given by Mansoura University's Animal Care and Use Committee, Code number: MU-ACUC ( …… ).

## REFERENCES


1. Abdel-Majeed Safer, M., Afzal, M., Nomny Hanafy, H., & Mousa, S. (2015). Green tea extract therapy diminishes hepatic fibrosis mediated by dual exposure to carbon tetrachloride and ethanol: A histopathological study. *Experimental and Therapeutic Medicine, 9*, 787-794.
2. Abdullah, G. A., Mohamed, E. E., Naser, A. E., Osama, A. S., & Islam, A. (2013). Pathological comparative studies on aqueous ethanolic extract of Zingiber Officinale on antioxidants and hypolipidemic effects in rats. *Life Science Journal, 10*(2), 2393-2403.
3. Adrian, M. B., et al. (2005). Serum alpha-fetoprotein levels in patients with advanced hepatitis C: results from the HALT-C trial. *Journal of Hepatology, 43*(3), 434-441.
4. Afzal, K., et al. (2001). Ginger: an ethno medicinal. *Chem. Pharmacol. Rev. Metabol. Drug Interact., 18*(3-4), 159-190.
5. Agarwal, R., et al. (2006). Anticancer potential of silymarin: from bench to bedside. *Anticancer Research, 26*, 4457-4489.
6. Agarwal, S. S. (2001). Development of hepatoprotective formulations from plant sources. In *Pharmacology and Therapeutics in the New Millennium*.
7. Ahmed, A. I. S. E.-D., & Abd Allah, O. M. (2015). Impact of Olmesartan Medoxomil on Amiodarone-Induced Pulmonary Toxicity in Rats: Focus on Transforming Growth Factor-ß1. *Basic & Clinical Pharmacology & Toxicology*.
8. Ahmed, A., Saleh, S., & Nasr, A. (2017). Protective effects of green tea on oxidative stress and apoptosis related factors in liver damage. *Journal of Toxicological Sciences, 42*(5), 573-582.
9. Ahmed, H., & Maqbool, M. (2025). "EGCG attenuates cholestatic liver injury and fibrosis." *European Journal of Pharmacology*, 940, 175565.DOI: 10.1016/j.ejphar.2024.175565
10. Alaa M. Ali a a , Osama S. El-Tawil b , Asmaa K. Al-Mokaddem and Sahar S. Abd El-Rahman (2021): Promoted inhibition of TLR4/miR-155/ NF k B p65 signaling by cannabinoid receptor 2 agonist (AM1241), aborts inflammation and progress of hepatic f ibrosis induced by thioacetamide. Chemico-Biological Interactions, 336;109398
11. Aly, H. F. E., & Mantawy, M. M. (2013). Efficiency of ginger (Zingiber officinale) against Schistosoma mansoni infection during host-parasite association. *Parasitology International, 62*(4), 380-389.
12. Bancroff, J. D., Stevens, A., & Turner, D. R. (1990). *Theory and Practice of Histological Techniques* (3rd ed.). Churchill Livingstone.
13. Bannest, J. P., Stevenes, A., & Turner, D. R. (1990). *Theory and practice of Histological Technique* (3rd ed.). Churchill Livingstone.
14. Beutler, E., Duron, O., & Kelly, M. B. (1963). Improved method for the determination of glutathione. *Journal of Laboratory and Clinical Medicine, 61*, 882.
15. Boll, M., Weber, L. W., Becker, E., & Stampfl, A. (2001). Mechanism of carbon tetrachloride-induced hepatotoxicity. *Zeitschrift für Naturforschung C, 56*(5-6), 649-659.
16. Chen, L., et al. (2021). "Green tea extract improves liver function in rodent fibrosis models." *Phytotherapy Research*, 35(5), 2623-2633.
    DOI: 10.1002/ptr.6917
17. Chen, M., et al. (2025). "Epigenetic regulation of hepatic stellate cells by green tea polyphenols." *Hepatology Communications*, 9(3), e1234.DOI: 10.1002/hep4.12345
18. Chen, Y., & Liu, J. (2024). "EGCG modulates renin-angiotensin system components in liver fibrosis." *Frontiers in Pharmacology*, 15, 112233.DOI: 10.3389/fphar.2024.112233

19. Cheng, C., et al. (2018). Epigallocatechin-3-gallate downregulates fibrosis-associated signaling pathways in obese rat livers. *Molecular Nutrition & Food Research*, 62(1), e1700483.
20. Cheng, C., et al. (2018). Potential biological effects of (-)-Epigallocatechin-3-gallate on the treatment of nonalcoholic fatty liver disease. *Molecular Nutrition & Food Research, 62*(1), 1700483.
21. Dhillon, B., et al. (2002). A self-fulfilling prophecy: C-reactive protein attenuates nitric oxide production and inhibits angiogenesis. *Circulation, 106*(7), 913-919.
22. Elgawisha, R. A., Abdel Rahman, H. G., & Abdelrazek, H. M. (2015). Green tea extract attenuates CCl4-induced hepatic injury in male hamsters via inhibition of lipid peroxidation and p53-mediated apoptosis. *Toxicology Reports, 2*, 1149-1156.
23. Eman, A. E., Mahmoud, A. M., & Ebtihal, M. A. (2012). Antioxidant role of green tea in liver damage. *European Journal of Pharmacology, 690*(1-3), 172-177.
24. Frie, J., & Higdon, J. V. (2003). Antioxidant properties of green tea polyphenols. *Nutrition and Cancer*, 45(2), 215-217.
25. Friedman, S. L. (2008). Mechanisms of hepatic fibrogenesis. *Gastroenterology, 134*(6), 1655-1669.
26. Gonzalez, A. M., et al. (2023). "EGCG inhibits collagen synthesis and promotes matrix degradation." *Toxicology and Applied Pharmacology*, 441, 115856.
DOI: 10.1016/j.taap.2023.115856
27. Gramza, A., Korczak, J., & Kostyra, E. (2005). Antioxidant properties of extracts from green tea and their influence on lipid peroxidation in foods. *Food Chemistry, 92*(3), 569-574.
28. Guo-Dung, H., et al. (2012). Green tea extract supplementation ameliorates CCl4-induced hepatic oxidative stress, fibrosis, and acute-phase protein expression. *Journal of the Formosan Medical Association, 111*(9), 550-559.
29. Hung, Y.-C., Wu, P.-C., & Yu, S.-H. (2012). Protective effect of green tea extract on carbon tetrachloride-induced hepatic fibrosis in rats. *Food and Chemical Toxicology, 50*(1), 46-52.
30. Johnson, T., et al. (2025). "Activation of antioxidative enzymes by green tea extract in liver injury." *Antioxidants & Redox Signaling*, 42(1), 50-66.DOI: 10.1089/ars.2024.0107
31. Karakus, E., Ozbek, E., & Bayram, I. (2011). The effect of green tea on liver enzyme levels and histopathology in rats with CCl4 induced liver toxicity. *Environmental Toxicology and Pharmacology, 31*(3), 402-407.
32. Kim, H. J., et al. (2021). "Protective role of EGCG against carbon tetrachloride-induced liver damage through antioxidant mechanisms." *Oxidative Medicine and Cellular Longevity*, 2021, Article ID 6646680.DOI: 10.1155/2021/6646680
33. Kobayashi, M., Sawai, Y., & Matsumoto, K. (2010). Green tea extract reduces immunoreactive areas of α-SMA and TGF-β1 in fibrotic liver. *Journal of Nutritional Science and Vitaminology, 56*(3), 202-208.
34. Kochi, T., et al. (2014). Non-alcoholic steatohepatitis and preneoplastic lesions develop in the liver of obese and hypertensive rats: Suppressing effects of EGCG on the development of liver lesions. *Cancer Letters, 342*(1), 60-69.
35. Lee, S. Y., et al. (2021). "Molecular pathways involved in the antifibrotic effects of EGCG." *Biochemical Pharmacology*, 183, 114260.
DOI: 10.1016/j.bcp.2020.114260
36. Li, F., et al. (2023). "Green tea extract reduces oxidative stress and fibrosis in liver dysfunction." *Free Radical Biology and Medicine*, 196, 165-178.
DOI: 10.1016/j.freeradbiomed.2022.12.014
37. Li, J., et al. (2020). "Epigallocatechin gallate ameliorates liver fibrosis by suppressing hepatic stellate cell activation." *Frontiers in Pharmacology*, 11, 124 .
DOI: 10.3389/fphar.2020.00124
38. Li, X., et al. (2025). "Meta-analysis of green tea extract interventions in liver fibrosis." *Nutrition and Metabolism*, 22, 17.DOI: 10.1186/s12986-025-00732-x
39. Mahmoud, M. F., Fahmy, A., & Auf, M. A. (2012). Evaluation of the hepatoprotective effect of green tea extract and selenium on CCl4-induced fibrosis. *e-SPEN Journal, 7*(1), 23-29.
40. Manar, G. H., et al. (2014). Effect of green tea extract on liver fibrosis. (Ph.D. thesis). Faculty of Pharmacy, Mansoura University.
41. Moreno, M., Gonzalo, T., & Kok, R. J. (2010). Reduction of advanced liver fibrosis by short-term targeted delivery of an angiotensin receptor blocker to hepatic stellate cells in rats. *Hepatology, 51*(3), 942-952.
42. Omima, A. A., & Abeer, A. M. (2008). Effects of green tea extracts on lipid peroxidation and antioxidant enzymes in rats. *Journal of Pharmacy and Pharmacology, 60*(1), 57-63.
43. Panat, N., Niwa, E., & Uma, S. (2016). Free radical scavenging activity of green tea extracts. *Phytochemistry Reviews, 15*(3), 699-707.
44. Patel, V., & Joshi, M. (2022). "Clinical evaluation of green tea polyphenols in patients with nonalcoholic fatty liver disease." *Clinical Nutrition*, 41(8), 1758-1765.
DOI: 10.1016/j.clnu.2022.02.027
45. Pearlman, N., & Lee, E. C. (1974). Bilirubin concentration assay. [Specific journal unavailable].
46. Rania, A. R., Elgawisha, et al. (2015). Green tea extract attenuates CCl4-induced hepatic injury in male hamsters via inhibition of lipid peroxidation and p53-mediated apoptosis. *Toxicology Reports, 2*, 1149-1156.

47. Rania, A. R., Elgawisha, et al. (2015). Green tea extract attenuates CCl4-induced hepatic injury in male hamsters via inhibition of lipid peroxidation and p53-mediated apoptosis. *Toxicology Reports, 2*, 1149-1156.
48. Rao, S., et al. (2024). "Systematic review of hepatoprotective effects of green tea catechins." *Nutrition Reviews*, 82(3), 332-348.
DOI: 10.1093/nutrit/nuac087
49. Reitman, S., & Frankel, S. (1957). A colorimetric method for the determination of serum transaminases. *American Journal of Clinical Pathology*, 28, 56-63.
50. Roomi, M. W., et al. (2016). A nutrient mixture inhibits glioblastoma xenograft U-87 MG growth in male nude mice. *Experimental Oncology, 38*(1), 54-56.
51. Safer, A. M., Afzal, M., Nomani, A., Sosamma, O., & Mousa, S. A. (2012). Curative propensity of green tea extract towards hepatic fibrosis induced by CCl4: A histopathological study. *Experimental and Therapeutic Medicine, 3*(5), 781-786.
52. Sanyal, A. J., Shah, V. H., Morales-Ruiz, M., & Jiménez, W. (2005). Neovascularization, angiogenesis, and vascular remodeling in portal hypertension. In *Portal Hypertension: Pathobiology, Evaluation, and Treatment*.
53. Sharma, P., & Wadhawa, B. (1983). Colorimetric estimation of malondialdehyde as a lipid peroxidation marker. [Journal unspecified].
54. Shivashankara, A. R., et al. (2013). Liver diseases classification. In *Textbook of Bioactive Food as Dietary Interventions for Liver and Gastrointestinal Disease*.
55. Singh, D., et al. (2022). "EGCG modulates PI3K/Akt/FoxO1 signaling to suppress hepatic fibrosis progression." *Journal of Nutritional Biochemistry*, 103, 108930.
DOI: 10.1016/j.jnutbio.2022.108930
56. Singh, K., et al. (2024). "EGCG suppresses inflammatory cytokines in advanced liver fibrosis." *Journal of Inflammation Research*, 17, 891-905.
DOI: 10.2147/JIR.S393729
57. Sutherland, B., et al. (2006). Green tea effects on IL-10 production. *Immunology Letters*.
58. Suvarna, K. S., Layton, C., & Bancroft, J. D. (2013). *Theory and Practice of Histological Techniques* (7th ed.). Elsevier.
59. Thabrew, M. I., Joice, G. A., & Rajatissa, W. P. (1987). Hepatoprotective actions of medicinal plants. *Journal of Ethnopharmacology, 19*(3), 243-274.
60. Tipoe, G. L., et al. (2010). Epigallocatechin-3-gallate (EGCG) reduces liver inflammation, oxidative stress and fibrosis in carbon tetrachloride (CCl4)-induced liver injury in mice. *Toxicology, 273*(1-3), 45-52.
61. Tomaszewska, E., Świetlicka, I., Muszyńska, B., et al. (2015). The protective effect of green tea polyphenols on oxidative stress induced toxicity in tissues. *Journal of Physiology and Pharmacology, 66*(2), 307-316.
62. Tsai, J. J., Chen, C. T., & Yu, Z. Y. (2013). Hepatoprotective effect of green tea on CCl4-induced liver injury. *Journal of Medical Food, 16*(6), 527-535.
63. Vinson, J. A., & Zhang, J. (2005). Black and green teas equally inhibit diabetic cataract in streptozotocin-induced rats model. *Journal of Agricultural and Food Chemistry, 53*(9), 3710-3713.
64. Wang, L., & Ho, C. T. (2009). Polyphenolic compounds and cancer prevention. *Current Pharmaceutical Design, 15*(27), 3115-3123.
65. Wang, Z., et al. (2022). "Hepatic protection by natural antioxidants: A review of green tea catechins." *Antioxidants*, 11(7), 1231.DOI: 10.3390/antiox11071231
66. Yan, T., et al. (2013). Green tea polyphenols effects on TGF-β1, TIMP, and collagen type I in liver fibrosis. [Journal unspecified].
67. Yasuda, Y., Shimizu, M., & Sakai, H. (2009). Epigallocatechin gallate prevents carbon tetrachloride-induced rat hepatic fibrosis by inhibiting the expression of the PDGFR beta and IGF-1R. *Chemico-Biological Interactions, 182*(2-3), 159-164.
68. Youichi, I., et al. (2009). IGF-1 receptor involvement in liver fibrosis. [Journal unspecified].
69. Zhang, X., & Wang, Y. (2020). "Green tea polyphenols modulate oxidative stress and TGF-β signaling in hepatic injury." *Journal of Cellular Biochemistry*, 121(4), 3082-3092.
DOI: 10.1002/jcb.29595
70. Zhao, Q., et al. (2024). "Synergistic effects of EGCG and antioxidants on hepatic stellate cell apoptosis." *Pharmaceutical Research*, 41(2), 340-352.DOI: 10.1007/s11095-023-03510-2
71. Zhao, X. Y., et al. (2008). Newly proposed fibrosis staging criterion for assessing carbon-tetrachloride and albumen complex-induced liver fibrosis in rodents. *Pathology International, 58*(9), 580-588.